Indian Journal of Chemistry
Vol. 65, July 2026, pp. 643-656
DOI: 10.56042/ijc.v65i7.22931

Theoretical investigation and prediction of ^{13}C and ^{1}H nuclear magnetic resonance chemical shifts in aromatic and new organometallic sandwich systems

Marc Fenzlaff* & Oliver Christoph Potzel

Department of Energy, Environmental and Process Engineering, Wilhelm Büchner University of Applied Science, 64295 Darmstadt, Germany

E-mail: marc.fenzlaff@wb-fernstudium.de, marcfenzlaff@gmail.com, oliver.potzel@wb-fernstudium.de

Received 20 August 2025; accepted (revised) 3 July 2026

This study evaluates a density functional theory (DFT)-based workflow for the prediction of ^{13}C and ^{1}H nuclear magnetic resonance (NMR) chemical shifts in aromatic and organometallic systems. Aromatic reference compounds, namely benzene, toluene, nitrobenzene, aniline and phenol, have been investigated at the B3LYP/TZVP level of theory using the Gauge-Including Atomic Orbital (GIAO) method and implicit chloroform solvation. The calculated chemical shifts show strong agreement with experimental reference data, with coefficients of determination above 0.98. Linear regression-based scaling has further reduced systematic deviations. To assess the transferability of the computational protocol to metal-containing systems, three additional organometallic benchmark compounds with published experimental ^{13}C and ^{1}H NMR data have been investigated: ferrocene, acetylferrocene and lithium cyclopentadienide. These compounds represent complementary organometallic bonding motifs, including sandwich complexes, a substituted ferrocene derivative with chemically distinct carbon and proton environments, and a lithium-containing cyclopentadienyl system. The workflow has been subsequently applied to pentaisopropylcyclopentadienyl-lithium ($Cp^{iPr5}Li$ (A)), pentaisopropylcyclopentadienyl-aluminium ($Cp^{iPr5}Al$ (B)), and a lithium-aluminium heterobimetallic dimetallocene ($Cp^{iPr5}Al–LiCp^{iPr5}$ (C)). For these target systems, calculated ^{13}C and ^{1}H chemical shifts have been evaluated by cross-platform comparison using Gaussian 09 and ORCA 6.0.1. Gaussian and ORCA have yielded closely matching predictions for the carbon and proton chemical shifts of compounds A and B, supporting the numerical reproducibility of the computational workflow. A comparison between the TZVP and QZVP basis sets has shown that QZVP substantially increased computational cost without improving predictive accuracy for the investigated aromatic reference systems. Overall, the results support B3LYP/TZVP/GIAO as an efficient computational protocol for the prediction and interpretation of ^{13}C and ^{1}H NMR chemical shifts in structurally diverse organic and organometallic systems.

Keywords: Gaussian, ORCA, B3LYP, TZVP, DFT, GIAO method, NMR chemical shifts

Nuclear Magnetic Resonance (NMR) spectroscopy is one of the most powerful analytical techniques for molecular structure determination in organic, inorganic and bioorganic chemistry[1]. Chemical shifts provide detailed information on the local electronic environments of nuclei and thereby enable atom-level structural interpretation. However, reliable prediction of NMR parameters for unknown, unstable or insufficiently characterised compounds remains challenging, particularly when experimental spectra are unavailable, incomplete or difficult to assign. This is especially relevant for recently reported Li/Al heterobimetallic systems with unusual bonding situations, for which computational NMR analysis can provide complementary structural information[2].

Quantum-chemical methods have become valuable tools for complementing experimental NMR analysis[3,4]. Among these methods, DFT is widely used because it provides a favourable balance between computational efficiency and predictive accuracy[5]. In combination with the GIAO formalism, DFT enables the calculation of magnetic shielding tensors in a manner that is independent of the chosen origin of the external magnetic field[5]. Consequently, GIAO-based DFT calculations are commonly applied for the prediction and interpretation of ^{13}C and ^{1}H NMR chemical shifts[5].

The predictive performance of calculated chemical shifts depends strongly on several methodological factors, including the exchange-correlation functional, basis set, molecular geometry, conformational sampling and treatment of solvent effects[5–8]. General-purpose triple-zeta basis sets such as TZVP are frequently used in practical NMR calculations because they offer a reasonable compromise between computational cost and accuracy[9,10]. Nevertheless, the

performance of a computational protocol should be evaluated against experimental reference data before it is applied to chemically more complex systems.

In the present study, a set of aromatic compounds was selected as an initial benchmark because these molecules are structurally rigid, electronically well-defined and associated with reliable experimental ^{13}C and ^{1}H NMR reference data. Benzene, toluene, nitrobenzene, aniline and phenol were therefore used to evaluate the intrinsic performance of the B3LYP/TZVP/GIAO protocol under controlled conditions. Their limited conformational flexibility and well-characterised substituent effects allow systematic deviations in calculated chemical shifts to be assessed without major contributions from aggregation phenomena, coordination effects or complex conformational equilibria.

This aromatic benchmark was not intended to directly represent organometallic bonding. Metal-containing compounds may differ substantially from aromatic molecules with respect to electronic structure, charge distribution, metal-ligand interactions and polarisation effects. Therefore, transferability of the computational workflow to metal-containing systems was additionally assessed using organometallic benchmark compounds with published experimental ^{13}C and ^{1}H NMR data. Ferrocene and acetylferrocene were selected as sandwich-type organometallic systems, whereas lithium cyclopentadienide was included as a lithium-containing cyclopentadienyl compound relevant to the lithium-containing target systems.

The validated workflow was subsequently applied to A, B and C (Ref. 2). These compounds represent recently reported organometallic systems with lithium-aluminium bonding situations. For compounds A and B, independent calculations using Gaussian 09 (Ref. 11) and ORCA[12,13] were performed to assess the numerical reproducibility of the calculated ^{13}C and ^{1}H chemical shifts across two quantum-chemical software packages. The corresponding cross-platform comparison was interpreted as an internal consistency check rather than as direct experimental validation. Based on the close numerical agreement obtained for A and B, compound C was subsequently calculated using ORCA[12,13].

The purpose of this study is therefore to evaluate the performance of the B3LYP/TZVP/GIAO approach for the prediction of ^{13}C and ^{1}H NMR chemical shifts across aromatic and organometallic systems. In addition to assessing the agreement between calculated and experimental data for aromatic and organometallic benchmark compounds, the study examines the numerical consistency of Gaussian- and ORCA-based predictions for the Li/Al target systems. A further comparison of TZVP and QZVP basis sets was performed to assess whether the increased computational cost associated with a larger basis set provides a meaningful improvement in predictive accuracy.

Theory

Nuclear Magnetic Resonance (NMR) spectroscopy is based on the interaction of nuclear magnetic moments with an external magnetic field. Nuclei possessing a non-zero spin generate a magnetic moment, which can interact with the applied magnetic field and absorb radiofrequency radiation at characteristic resonance frequencies. These resonance conditions depend not only on the intrinsic properties of the nucleus, such as its gyromagnetic ratio, but also on its electronic environment. The chemical shift is defined as the difference in resonance frequency relative to a reference compound and reflects the local shielding caused by the surrounding electron density[14].

The shielding constant, which underlies the chemical shift, is sensitive to subtle variations in molecular geometry and electronic structure. For this reason, theoretical prediction of NMR parameters requires accurate modeling of electron distributions. One of the most widely used approaches for this purpose is Density Functional Theory (DFT).

DFT simplifies the many-electron problem by focusing on the electron density rather than the wavefunction. According to the Hohenberg-Kohn theorems, all ground-state properties of a system are determined uniquely by its electron density[15]. The Kohn–Sham formulation introduces a set of non-interacting orbitals that reproduce the exact ground-state density, thereby making the problem computationally tractable. Exchange and correlation effects, which cannot be described exactly, are included through approximate functionals[16]. In this work, the hybrid functional B3LYP[17-20] is employed due to its well-documented performance across a range of systems, including organic and organometallic compounds.

For calculating magnetic properties such as chemical shielding tensors, the GIAO method is

used[5,21-24]. This formalism embeds the magnetic vector potential directly into the basic functions, making the results independent of the origin of the applied field. The GIAO approach is the current standard in NMR calculations and is implemented in most modern quantum chemistry software packages.

The choice of basis set is a critical factor in determining the accuracy of computed NMR parameters. Although specialized basis sets exist for shielding calculations, this study employs the TZVP basis set, which is widely used in literature[6,25] and offers a good compromise between accuracy and computational cost.

Solvent effects can influence the electronic structure and thus the chemical shift, particularly in polar or flexible molecules. In this work, solvation is modeled using the Polarizable Continuum Model (PCM)[26-29] with chloroform as the implicit solvent. This model treats the solvent as a continuous dielectric medium, surrounding the solute in a molecular-shaped cavity and accounting for polarization effects.

Together, the combination of the B3LYP functional, TZVP basis set, GIAO formalism and PCM solvation provides a robust framework for predicting NMR chemical shifts in both aromatic and organometallic systems. In the present study, the accuracy of this theoretical approach is assessed by comparing the calculated values with available experimental reference data for selected compounds.

Methodology

The molecular systems investigated in this study comprised three categories: five aromatic reference compounds with well-documented experimental ^{13}C and ^{1}H NMR data[30], three organometallic benchmark compounds with published experimental ^{13}C and ^{1}H NMR data[30,31], and three Li/Al target compounds. The aromatic compounds included benzene, toluene, nitrobenzene, aniline and phenol. The organometallic benchmark compounds were ferrocene, acetylferrocene and lithium cyclopentadienide. The Li/Al target compounds were A, B, and C (Ref. 2) (Fig. 1).

Initial molecular geometries were obtained from the PubChem database[32–37] where available. Structures not available from PubChem were constructed in Avogadro[38] and subjected to preliminary geometry optimisation to generate reasonable starting configurations. Geometry optimisations and frequency analyses were performed at the B3LYP/TZVP level of theory. The absence of imaginary frequencies was used to confirm that each optimised structure represented a local minimum on the potential-energy surface.

Nuclear magnetic shielding constants were calculated using the GIAO method. All computed shielding values were referenced to tetramethylsilane (TMS), which was calculated at the same level of theory. Relative chemical shifts in parts per million were obtained by subtracting the calculated absolute shielding constant of each nucleus from the corresponding calculated shielding constant of TMS. Solvent effects were included using the PCM with chloroform as the implicit solvent (dielectric constant $\varepsilon = 4.7113$). The integral equation formalism variant of PCM (IEFPCM) implemented in Gaussian was applied.

For the aromatic reference compounds and the organometallic benchmark compounds, calculated ^{13}C

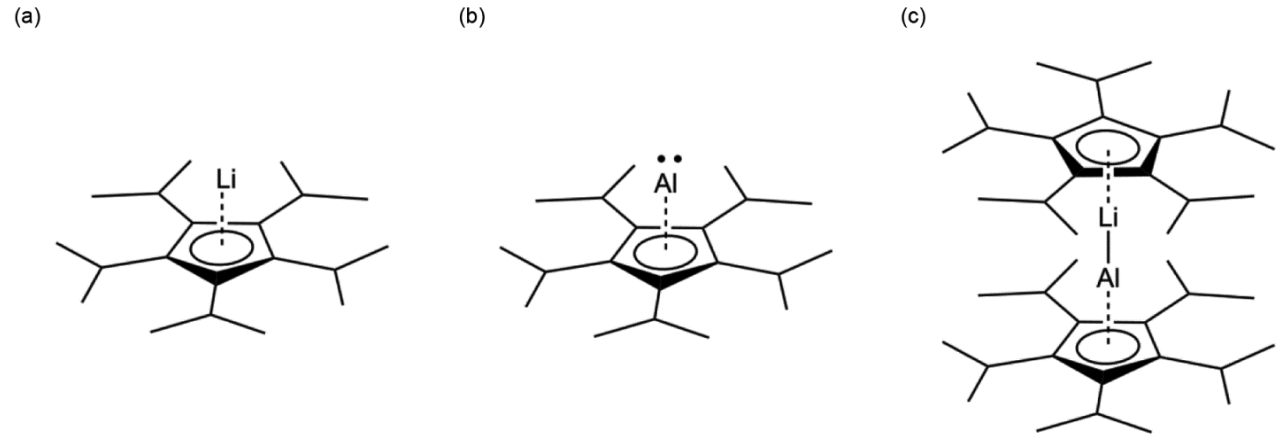

Fig. 1 — Structural visualizations of the three organometallic compounds A, B and the Li-Al heterobimetallic dimetallocene.

and ^{1}H chemical shifts were compared directly with published experimental values[30,31]. Ferrocene and acetylferrocene were included as sandwich-type organometallic reference compounds, whereas lithium cyclopentadienide was included as a lithium-containing cyclopentadienyl system relevant to the Li/Al target compounds. The structural model selected for lithium cyclopentadienide reflected the reported experimental species as closely as possible.

For the Li/Al target compounds A, B and C, the calculated ^{13}C and ^{1}H chemical shifts were not subjected to direct atom-by-atom comparison with experimental reference values. Instead, compounds A and B were independently calculated using Gaussian 09 (Ref. 11) and ORCA 6.0.1 (Ref. 12,13) to assess numerical reproducibility across quantum-chemical software packages. Compound C was subsequently calculated using ORCA based on the close numerical agreement obtained for A and B.

For datasets with complete experimental reference values, calculated chemical shifts were evaluated using linear regression, coefficients of determination (R^2), mean absolute error (MAE) and coefficient of variation (CV). Bland-Altman plots were generated to visualise systematic deviations between calculated and experimental values[39-41]. Simulated NMR spectra were generated by applying Lorentzian line shapes to calculated chemical shifts and were compared with experimental reference spectra where available[30,31].

Results and Discussion

The results of this study are presented in two parts: aromatic compounds and organometallic systems. Each group was evaluated for ^{13}C and ^{1}H NMR chemical shift predictions obtained using DFT-based methods. For aromatic compounds, the theoretical values were directly compared with experimental data from textbooks and spectral databases[31] to assess predictive performance. For the aromatic reference compounds and the organometallic benchmark systems, calculated ^{13}C and ^{1}H chemical shifts were directly compared with published experimental data. For the Li/Al target compounds A - B, calculated shifts were assessed by cross-platform comparison between Gaussian 09 and ORCA 6.0.1 as an internal consistency check. All results were obtained using Gaussian 09 at the B3LYP/TZVP level of theory and the analysis includes statistical evaluation and spectral simulation to support the interpretation.

Aromatic Compounds

^{13}C NMR Chemical Shifts

The ^{13}C NMR chemical shifts predicted at the B3LYP/TZVP level showed excellent agreement with the literature reference values[30]. Linear regression analysis comparing calculated and experimental chemical shifts yielded a regression equation of $y = 0.9305x + 4.3941$ with a coefficient of determination $R^2 = 0.9951$ (Fig. 2).

This indicates a strong linear relationship and low systematic deviation across the examined dataset of aromatic compounds. The largest deviation was observed for quaternary carbon atoms in proximity to strongly electron-donating or electron-withdrawing substituents. In particular, the hydroxyl-bearing carbon in phenol and the amino-substituted carbon in aniline showed deviations of up to 9 ppm. These findings are consistent with the known sensitivity of ^{13}C to local electronic effects and substitution patterns[42,43]. A Bland-Altman analysis further confirmed the robustness of the predictions (Fig. 3).

Most values fell within the limits of agreement defined as bias ± 1.96 SD and the mean deviation was approximately 4.8 ppm. This level of accuracy is well within the expected range for unscaled DFT-based ^{13}C NMR predictions. Simulated ^{13}C spectra of the aromatic compounds, including benzene, nitrobenzene and phenol, reflected the correct number and relative positioning of signals. After applying the regression analysis, the calculated spectra showed near-perfect alignment with experimental data, demonstrating the practical reliability of the

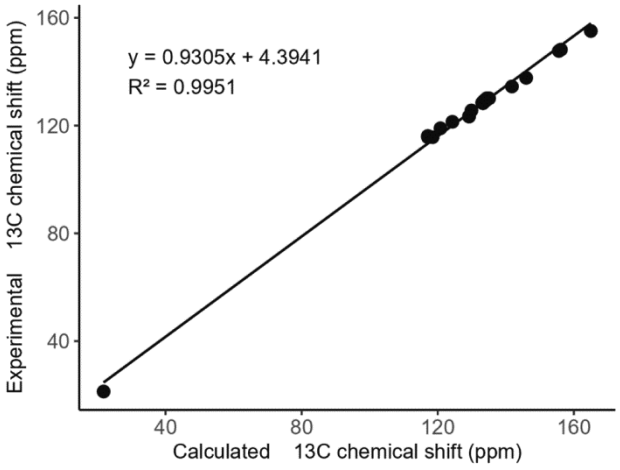

Fig. 2 — Correlation between calculated and experimental ^{13}C NMR chemical shifts at the B3LYP/TZVP level of theory. The linear regression (black line) indicates an excellent agreement and a minor systematic deviation across the dataset.

computational method for structure verification in substituted aromatics (Fig. 4).

^{1}H NMR Chemical Shifts

The ^{1}H NMR predictions also show strong consistency with literature and database values[30,31]. Linear regression between calculated and experimental chemical shifts yielded the equation $y = 1.0133x - 0.0039$ with a coefficient of determination $R^2 = 0.9976$ (Fig. 5).

This reflects a high degree of linear correlation, albeit with slightly more scatter than observed in the ^{13}C data. The mean absolute error was approximately 0.30 ppm. Notable deviations were observed for the methyl protons in toluene as well as exchangeable protons in functional groups such as NH_2 in aniline and OH in phenol. These discrepancies are likely due to solvent-dependent effects and hydrogen bonding, which are only partially represented in the implicit PCM solvent model. The Bland-Altman plot for ^{1}H shifts (Fig. 6) supports these observations. Most data points lie within the limits of agreement and the bias is low, indicating no major systematic over- or underestimation across the chemical shift range.

As with the ^{13}C results, the raw and scaled ^{1}H spectra were compared visually to literature values[30,31].

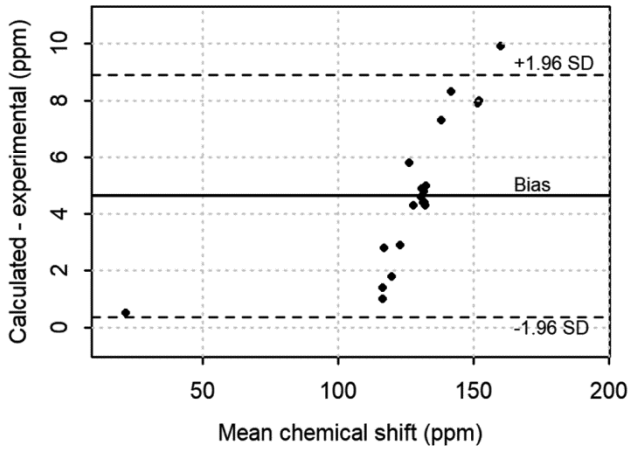

Fig. 3 — Bland-Altman plot for ^{13}C NMR chemical shifts predicted at the B3LYP/TZVP level: The plot shows the differences between calculated and experimental chemical shifts as a function of their mean values. The black line indicates the mean deviation (bias), while the dashed lines represent the limits of agreement (± 1.96 SD). Most values fall within the limits of agreement defined as bias ± 1.96 SD, demonstrating good agreement with minor systematic deviations.

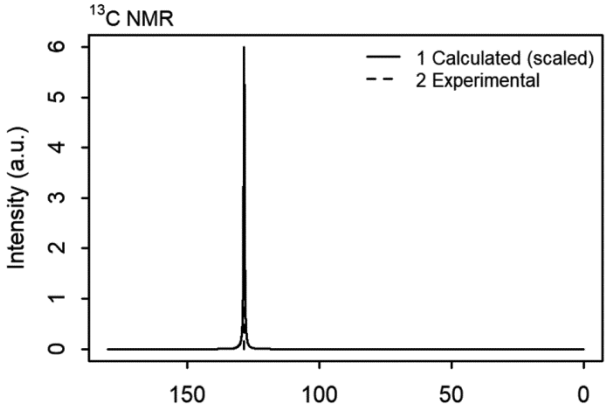

Fig. 4 — Scaled ^{13}C NMR spectrum of benzene: The calculated chemical shifts were scaled using the regression equation y = 0.9305x + 4.3941, resulting in a significantly improved agreement with experimental values. Peak positions are visualized with Lorentzian line shapes.

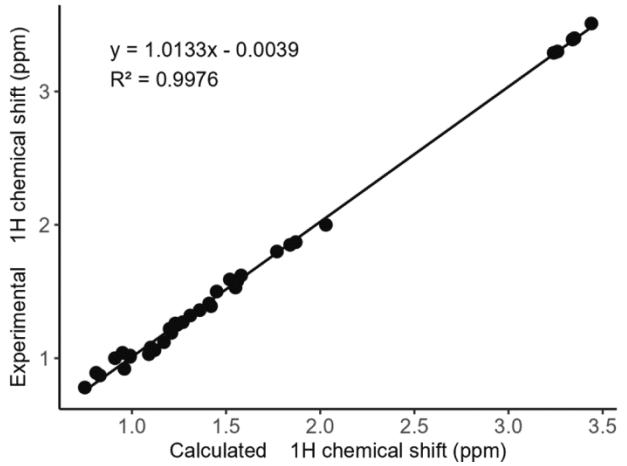

Fig. 5 — Correlation between calculated and experimental ^{1}H NMR chemical shifts at the B3LYP/TZVP level of theory. The red line represents the linear regression and indicates an excellent agreement and minimal systematic deviation.

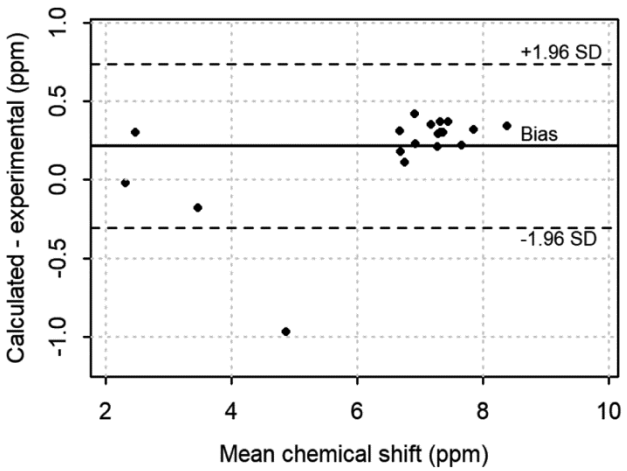

Fig. 6 — Bland-Altman plot illustrating the agreement between calculated and experimental ^{1}H NMR chemical shifts. The x-axis shows the mean of the calculated and experimental values, while y-axis shows their difference. The black line indicates the mean difference (bias) and the dashed lines represent the ± 1.96 standard deviation (SD) limits of agreement.

After linear correction, the predicted ^{1}H shifts closely matched the experimental signals (Fig. 7), confirming the suitability of the method for routine proton NMR prediction in aromatic compounds.

Organometallic Compounds

Organometallic Benchmark Systems

To assess the transferability of the B3LYP/TZVP/GIAO protocol to metal-containing compounds, three organometallic benchmark systems with published experimental ^{13}C and ^{1}H NMR data[30,31] were investigated: ferrocene, acetylferrocene and lithium cyclopentadienide. Ferrocene was selected as a classical sandwich complex, whereas acetylferrocene represents a structurally related but less symmetric derivative with a broader range of chemically distinct proton and carbon environments. Lithium cyclopentadienide was included as a lithium-containing cyclopentadienyl compound and therefore provides a relevant reference for the lithium-containing target systems.

For the combined organometallic benchmark dataset, calculated and experimental ^{13}C chemical shifts showed excellent agreement. Linear regression yielded a coefficient of determination of $R^2 = 0.9983$ and the regression equation $y = 0.9561x - 0.4556$ (Fig. 8).

The slope close to unity and the low intercept indicate that the B3LYP/TZVP/GIAO workflow reproduced the experimental ^{13}C chemical-shift scale of the investigated metal-containing compounds with only minor systematic deviation.

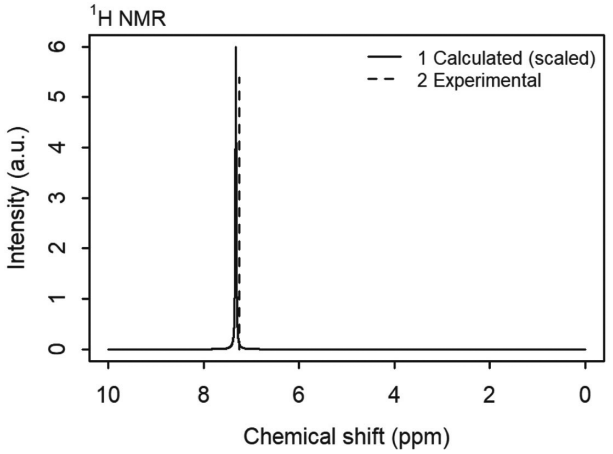

Fig. 7 — Scaled ^{1}H NMR spectrum of benzene: The simulated ^{1}H NMR spectrum is based on B3LYP/TZVP-calculated chemical shifts scaled using the regression equation y = 1.0133x - 0.0039. The experimental chemical shift shows excellent agreement with the scaled prediction, confirming the accuracy of applied correction.

Bland-Altman analysis further supported this result. The ^{13}C differences between calculated and experimental values were distributed around a small overall bias, and the majority of data points were located within the limits of agreement defined as bias ± 1.96 SD (Fig. 9). This indicates that no pronounced systematic deviation was observed across the investigated ^{13}C chemical-shift range.

The corresponding ^{1}H comparison showed a lower, but still clear, correlation between calculated and experimental chemical shifts ($R^2 = 0.8915$; Fig. 10).

The lower correlation was mainly associated with two resonances of acetylferrocene that deviated from the overall trend. These deviations may reflect the

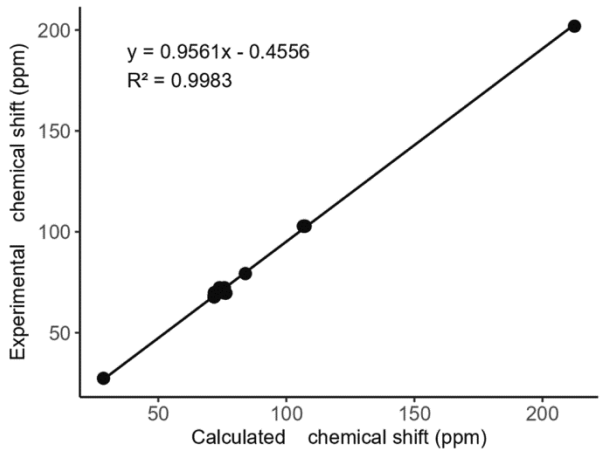

Fig. 8 — Correlation between calculated and experimental ^{13}C NMR chemical shifts for ferrocene, acetylferrocene and lithium cyclopentadienide at the B3LYP/TZVP/GIAO level of theory. The solid line represents the linear regression.

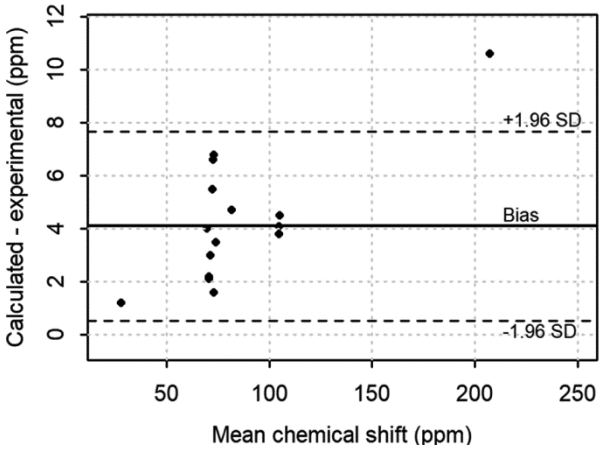

Fig. 9 — Bland-Altman plot for calculated and experimental ^{13}C NMR chemical shifts of ferrocene, acetylferrocene and lithium cyclopentadienide. The solid line represents the mean difference between calculated and experimental values, whereas the dashed lines indicate the limits of agreement defined as bias ± 1.96 SD.

greater sensitivity of proton chemical shifts to substituent-dependent shielding effects, molecular conformation and solvent-dependent contributions that are not fully captured by the implicit solvation model. The Bland-Altman plot for the ^{1}H benchmark dataset showed a broader distribution of differences than observed for ^{13}C chemical shifts, consistent with the lower regression coefficient. Nevertheless, most values remained within the limits of agreement defined as bias ± 1.96 SD (Fig. 11). Together, the regression and Bland-Altman analyses support the applicability of the B3LYP/TZVP/GIAO workflow for predicting ^{1}H chemical shifts in the investigated organometallic benchmark systems. These benchmark results provide external experimental support for the transferability of the protocol from aromatic compounds to selected metal-containing systems.

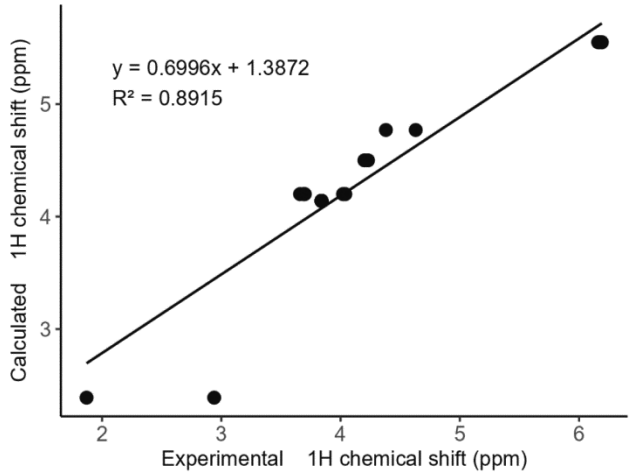

Fig. 10 — Correlation between calculated and experimental ^{1}H NMR chemical shifts for ferrocene, acetylferrocene and lithium cyclopentadienide at the B3LYP/TZVP/GIAO level of theory. The solid line represents the linear regression.

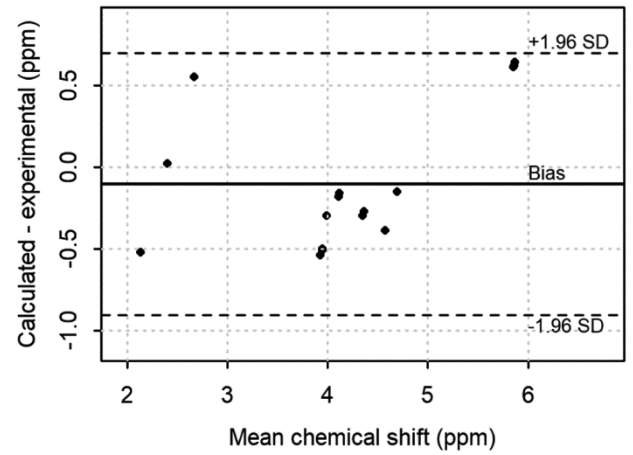

Fig. 11 — Bland-Altman plot for calculated and experimental ^{1}H NMR chemical shifts of ferrocene, acetylferrocene and lithium cyclopentadienide. The solid line represents the mean difference between calculated and experimental values, whereas the dashed lines indicate the limits of agreement defined as bias ± 1.96 SD.

Li/Al Target Systems

The Li/Al target systems investigated in this study were A, B and C (Ref. 2). Experimental multinuclear NMR spectra have been reported previously for selected compounds, including ^{13}C, ^{1}H, ^{7}Li and ^{27}Al NMR data. However, these spectra were not used for direct atom-by-atom quantitative validation of the calculated TMS-referenced ^{13}C and ^{1}H chemical shifts in the present work.

Instead, compounds A and B were independently calculated using Gaussian 09 and ORCA 6.0.1 to assess numerical reproducibility across two quantum-chemical software packages. The comparison was interpreted as an internal consistency check and not as a substitute for experimental validation.

^{13}C NMR Chemical Shifts

For compounds A and B, calculated ^{13}C chemical shifts obtained with Gaussian 09 and ORCA 6.0.1 showed excellent numerical agreement. Linear regression yielded the equation $y = 1.0090x + 0.5647$ with $R^2 = 0.9998$ (Fig. 12). The CVs across all calculated carbon shifts were below 2.5%, except for one aliphatic carbon atom in an isopropyl substituent.

^{1}H NMR Chemical Shifts

Similarly, calculated ^{1}H chemical shifts for compounds A and B showed close numerical agreement between Gaussian 09 and ORCA 6.0.1.

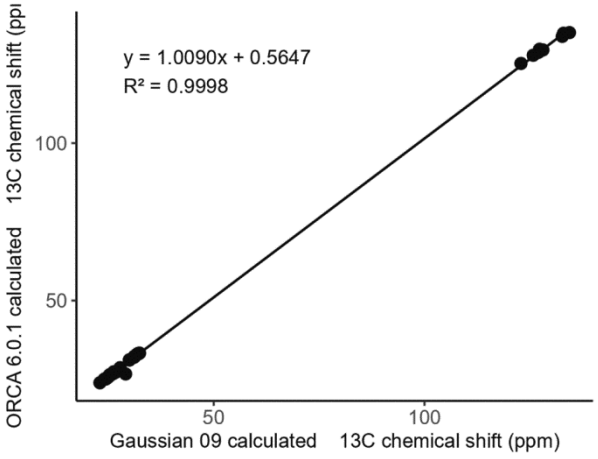

Fig. 12 — Correlation between Gaussian 09 and ORCA 6.0.1 calculated ^{13}C NMR chemical shifts for compounds A and B at the B3LYP/TZVP level of theory. The regression equation is y = 1.0090x + 0.5647, with R2 = 0.9998.

Regression analysis yielded $y = 1.0177x - 0.0205$, with $R^2 = 0.9982$ (Fig. 13).

The CVs across all protons were consistently low, with a mean CV of 0.98% and a maximum of 4.71%. The largest deviations were found for aliphatic protons, particularly those in methylene and isopropyl environments. These results underline the high level of agreement between Gaussian and ORCA, confirming the reproducibility of the predicted ^{1}H shifts across both software platforms.

The close agreement between the two software packages supports the numerical reproducibility of the computational implementation under comparable conditions. Based on this internal consistency check, subsequent calculations for the Li-Al heterobimetallic dimetallocene C were performed using ORCA.

The ^{13}C and ^{1}H chemical shifts obtained for the Li-Al heterobimetallic dimetallocene are summarized in Table 1.

To complement the NMR data, we next visualized the spatial distribution of electron density in the heterobimetallic Li-Al complex. Fig. 14 presents a 2D contour plot derived from the cube file with a ball-and-stick overlay; a zoomed-in panel directly below (Fig. 15) focuses on the metal centers to highlight local features of the coordination sphere.

Impact of QZVP on Computational Accuracy and Cost

To asses the potential accuracy gains from a larger basis set, a test calculation was performed for five

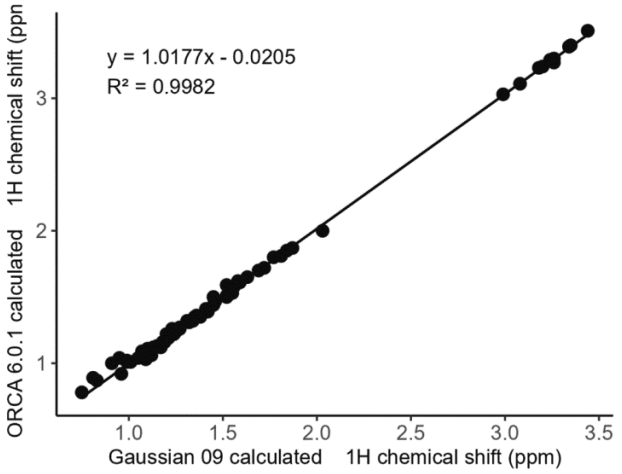

Fig. 13 — Correlation between Gaussian 09 and ORCA 6.0.1 calculated ^{1}H NMR chemical shifts for compounds A and B at the B3LYP/TZVP level of theory. The regression equation is y = 1.0177x – 0.0205, with R2 = 0.9982.

Table 1 — Calculated ^{13}C and ^{1}H Chemical Shifts for Li-Al Heterobimetallic Dimetallocene Using ORCA 6.0.1

C-Atom	Chemical Shift (δ, ppm)	H-Atom	Chemical Shift (δ, ppm)
2	129.0	9	0.87
3	124.8	10	0.95
4	127.7	11	1.31
5	129.1	13	1.89
6	128.2	14	1.31
7	33.2	15	1.04
8	25.5	18	1.20
12	28.6	19	0.99
16	32.5	20	1.78
17	26.4	22	0.84
21	28.8	23	1.14
25	32.0	24	1.54
26	26.9	27	1.05
30	30.8	28	1.26
34	33.1	29	1.70
35	27.8	31	0.69
39	25.9	32	1.34
43	31.8	33	1.14
44	25.5	36	0.94
48	28.6	37	1.26
60	25.9	38	1.77
61	24.9	40	1.48
63	26.9	41	0.98
65	32.3	42	1.00
73	24.5	45	1.03
74	31.1	46	1.50
76	134.9	47	1.18
77	25.6	49	0.96
78	134.4	50	1.20
85	30.1	51	1.50
86	135.0	52	3.20
87	31.2	53	3.36
89	130.0	54	3.27
92	135.7	55	3.28
95	32.9	56	3.20
96	23.7	57	1.25
98	32.1	58	1.08
99	26.7	59	1.39
105	27.2	62	3.26
107	25.0	64	1.15
–	–	66	1.63
–	–	67	1.14
–	–	68	1.06
–	–	69	1.02
–	–	70	1.46
–	–	71	1.41
–	–	72	1.24
–	–	75	1.59
–	–	79	2.36
–	–	80	3.11
–	–	81	1.08

(*Contd.*)

Table 1 — Calculated ^{13}C and ^{1}H Chemical Shifts for Li-Al Heterobimetallic Dimetallocene Using ORCA 6.0.1 (*Contd.*)

C-Atom	Chemical Shift (δ, ppm)	H-Atom	Chemical Shift (δ, ppm)
–	–	82	1.01
–	–	83	1.26
–	–	88	1.08
–	–	90	0.89
–	–	91	3.02
–	–	93	3.19
–	–	94	0.96
–	–	97	1.03
–	–	100	3.23
–	–	101	1.21
–	–	102	1.00
–	–	103	1.30
–	–	104	0.99
–	–	106	1.30
–	–	108	1.76
–	–	109	1.57
–	–	110	1.70
–	–	111	1.11
–	–	112	1.21

aromatic reference compounds like above and TMS using the QZVP basis set[44]. The results were compared to those obtained with the TZVP basis set under otherwise identical conditions (B3LYP/GIAO, PCM in chloroform). For ^{13}C NMR chemical shifts, the TZVP calculations yielded a mean absolute error (MAE) of 4.64 ppm with an R^2 value of 0.9951 while the QZVP basis set resulted in a higher MAE of 8.94 ppm despite a comparable correlation (R^2 = 0.9956). For ^{1}H shifts, TZVP produced a MAE of 0.3 ppm (R^2 = 0.9976), compared to 0.41 ppm (R^2 = 0.9902) for QZVP. These findings indicate no improvement in predictive accuracy when switching from TZVP to QZVP for the studied systems. In terms of computational costs, QZVP proved to be orders of magnitude more demanding. For example, the total computation time for benzene increased from 33 minutes (TZVP) to 1374 minutes (QZVP) and for toluene from 84 minutes to 5451 minutes. Across all test molecules QZVP runtimes were between ~ 30- and 100-fold longer than those of TZVP. A direct

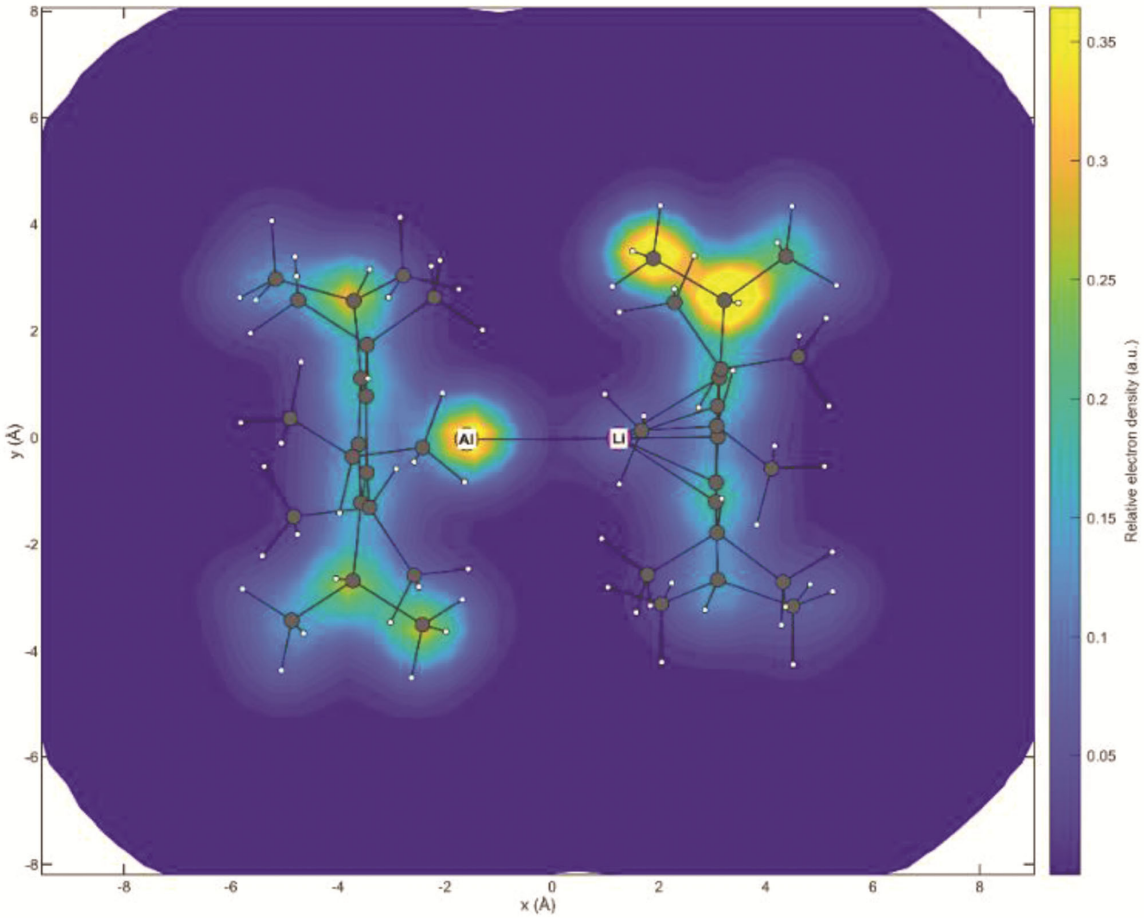

Fig. 14 — Overview 2D electron-density contour plot of the Li-Al heterobimetallic complex in the molecular x-y plane. A ball-and-stick overlay marks atomic positions, with Li and Al labeled. Contour spacing and the color scale match the bar at right; axes in angström[40].

comparison of calculated chemical shifts for ^{13}C and ^{1}H (Table 2 and Table 3) confirms the high agreement between TZVP and QZVP results with only minor numerical deviations. However, given the substantial increase of computation time and the lack of accuracy improvement, the use of QZVP was deemed inefficient for the present study. All subsequent NMR calculations were therefore performed using the TZVP basis set.

The overall comparison of TZVP and QZVP performance is summarized in Fig. 16. The diagram compiles total computation times per molecule on a logarithmic scale, the runtime ratio (QZVP/TZVP) and the corresponding accuracy metrics – mean absolute error (MAE) and coefficient of determination (R^2) – for both ^{13}C and ^{1}H nuclei. This visual summary highlights the substantial increase in computational cost when using QZVP, contrasted with the marginal and inconsistent changes in predictive accuracy compared to TZVP.

General Discussion

Across the aromatic and organometallic benchmark systems, the B3LYP/TZVP/GIAO protocol with PCM solvation provided reliable predictions of ^{13}C and ^{1}H NMR chemical shifts. For the aromatic reference compounds, calculated shifts showed close agreement with experimental data, and linear regression-based scaling further reduced systematic deviations. This demonstrates that the applied workflow is suitable for practical spectral interpretation and assignment of structurally related compounds.

The additional organometallic benchmark systems, ferrocene, acetylferrocene and lithium cyclopentadienide, provided external experimental support for the transferability of the computational

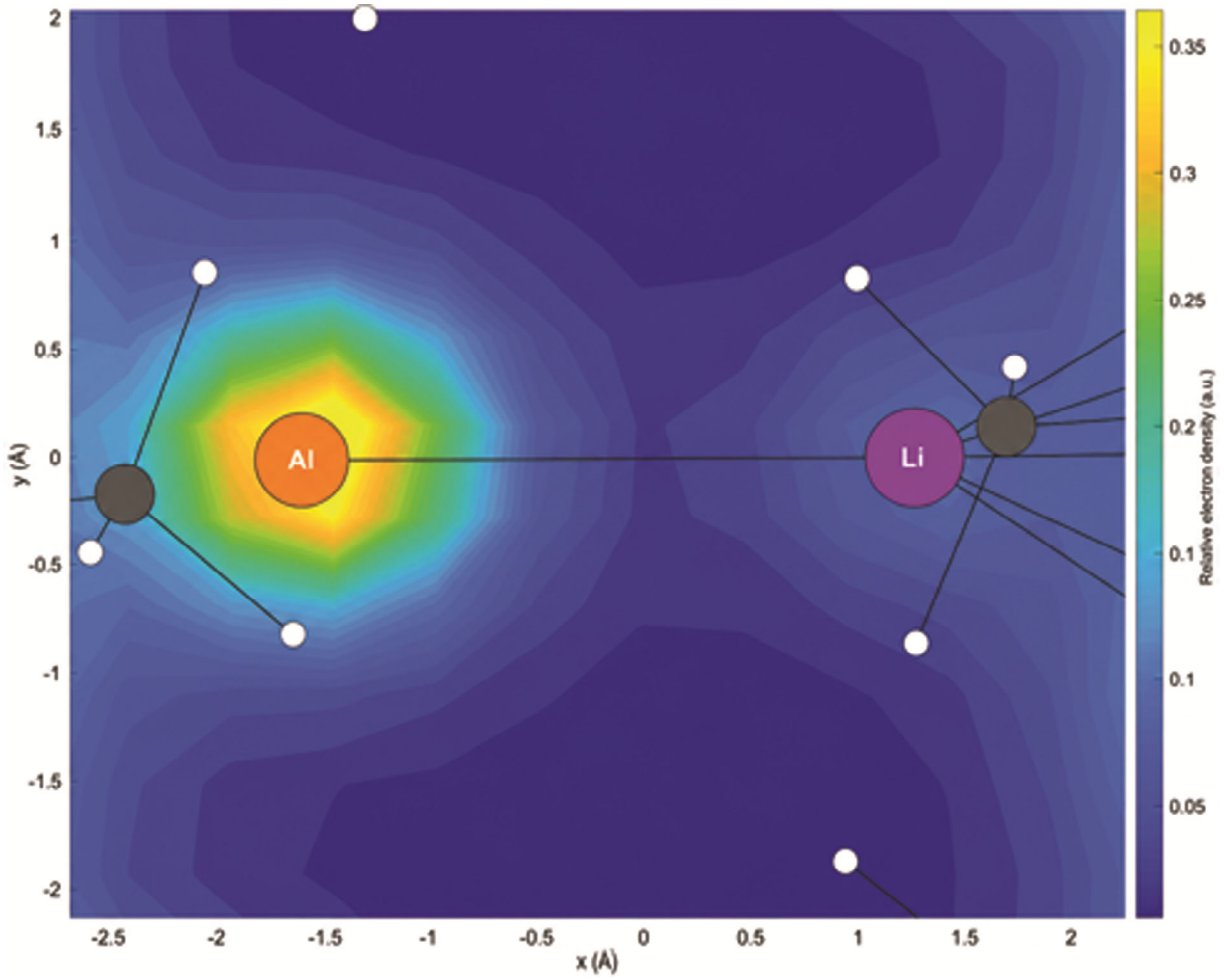

Fig. 15 — 2D electron-density contour map for the heterobimetallic Li-Al complex. Filled contours (colorbar at right) indicate relative electron density; a ball-stick overlay marks atomic positions, with the metal centers annotated (Al left, Li right). Axes are in angström; the plot is rendered from the cube data in the molecular (x-y) plane, showing the stronger density localization around Al compared to Li (Ref. 40).

Table 2 — Comparison of Calculated ^{13}C Chemical Shifts for Aromatic Compounds Using TZVP and QZVP Basis Sets With Corresponding Experimental Values in δ, ppm.

Compd	C-Atom	TZVP (δ, ppm)	QZVP (ppm)	Experimental (δ, ppm)
Benzene	1	133.3	137.7	128.5
	2	133.3	137.7	128.5
	3	133.3	137.7	128.5
	4	133.3	137.7	128.5
	5	133.3	137.7	128.5
	6	133.3	137.7	128.5
Toluene	1	146.0	150.6	137.7
	2	133.7	138.2	129.3
	3	133.7	138.2	129.3
	4	21.8	24.4	21.3
	5	133.1	137.5	128.5
	6	133.1	137.5	128.5
	7	129.9	134.0	125.6
Nitrobenzene	4	156.2	159.3	148.2
	5	129.2	134.1	123.4
	6	129.2	134.1	123.4
	7	134.1	138.4	129.3
	8	134.1	138.4	129.3
	9	141.8	146.3	134.5
Aniline	2	155.6	159.6	147.7
	3	117.1	121.6	116.1
	4	117.1	121.6	116.1
	5	134.2	138.8	129.8
	6	134.2	138.8	129.8
	7	120.8	124.9	119.0
Phenol	2	165.0	169.6	155.1
	3	117.1	121.5	115.7
	4	118.5	122.7	115.7
	5	134.4	139.0	130.1
	6	135.1	139.6	130.1
	7	124.3	128.2	121.4

Table 3 — Comparison of Calculated ^{1}H Chemical Shifts for Aromatic Compounds Using TZVP and QZVP Basis Sets With Corresponding Experimental Values (Exp.) in ppm.

Compd	H-Atom	TZVP (δ, ppm)	QZVP (δ, ppm)	Experimental (δ, ppm)
Benzene	7	7.63	7.77	7.26
	8	7.63	7.77	7.26
	9	7.63	7.77	7.26
	10	7.63	7.77	7.26
	11	7.63	7.77	7.26
	12	7.63	7.77	7.26
Toluene	8	7.47	7.59	7.17
	9	7.47	7.59	7.17
	10	2.30	2.37	2.32
	11	2.30	2.37	2.32
	12	2.62	2.38	2.32
Nitrobenzene	13	7.51	7.64	7.21
	14	7.51	7.64	7.21
	15	7.38	7.52	7.17
	10	8.55	8.86	8.21
	11	8.55	8.86	8.21
	12	7.77	7.93	7.55
	13	7.77	7.93	7.55
	14	8.01	8.15	7.69
Aniline	8	6.83	6.94	6.52
	9	6.83	6.94	6.52
	10	7.35	7.48	7.00
	11	7.35	7.48	7.00
	12	6.78	6.97	6.60
	13	3.37	3.68	3.55
	14	3.37	3.68	3.55
Phenol	8H	6.81	6.99	6.70
	9H	7.12	7.22	6.70
	10H	7.43	7.58	7.14
	11H	7.51	7.65	7.14
	12H	7.04	7.22	6.81
	13H	4.38	4.66	5.35

protocol to metal-containing compounds. In particular, the excellent agreement obtained for ^{13}C chemical shifts indicates that the B3LYP/TZVP/GIAO approach can reproduce the experimental carbon chemical-shift scale of the investigated organometallic systems with only minor systematic deviation. The corresponding ^{1}H results showed a lower, but still meaningful, level of agreement, reflecting the greater sensitivity of proton chemical shifts to local substituent effects, molecular geometry and solvent-dependent contributions.

The comparative basis-set evaluation showed that the larger QZVP basis set did not provide a meaningful improvement in predictive accuracy for the investigated aromatic reference systems. TZVP yielded lower mean absolute errors for both ^{13}C and ^{1}H chemical shifts, while the coefficients of determination remained comparable for both basis sets. At the same time, QZVP calculations required substantially longer runtimes, in several cases exceeding the TZVP runtimes by more than one order of magnitude. The combination of lower computational cost and comparable or improved agreement with experiment therefore supports the use of TZVP as the preferred basis set for the present workflow.

For the Li/Al target compounds A and B, direct atom-by-atom quantitative validation against experimental ^{13}C and ^{1}H chemical shifts was not performed. Instead, Gaussian 09 and ORCA 6.0.1 calculations were compared as an internal consistency check. The near-linear agreement between the calculated ^{13}C and ^{1}H chemical shifts obtained with both software packages demonstrates high numerical reproducibility under comparable computational conditions. This cross-platform agreement should not

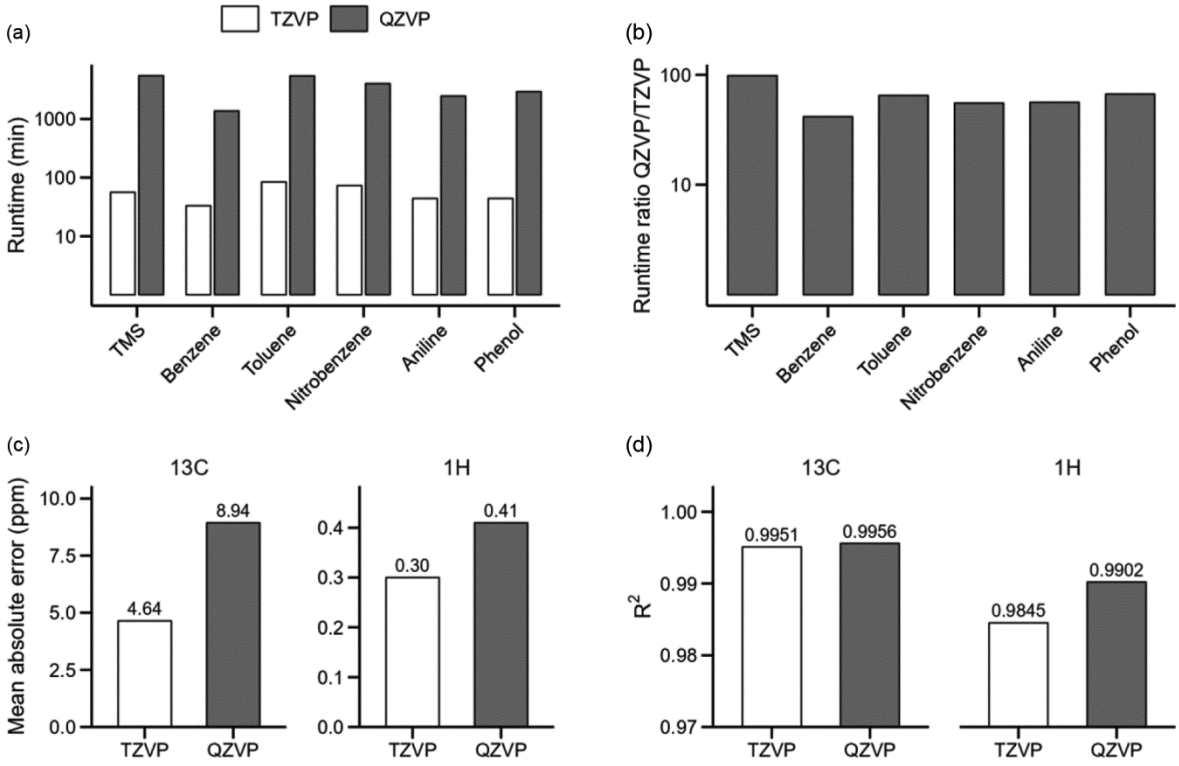

Fig. 16 — (a) Total computation time per molecule on a logarithmic scale, highlighting the substantial runtime increase when using QZVP. (b) Runtime ratio (QZVP/TZVP) for each molecule, shown on a log scale. (c) Mean absolute error (MAE) as chemical shift (ppm) for carbon-13 and proton NMR predictions, comparing TZVP and QZVP. (d) Coefficient of determination (R2) for the same nuclei and basis sets, indicating similar correlation quality despite runtime differences.

be interpreted as direct proof of experimental accuracy; however, it supports the robustness of the computational implementation and justified the subsequent use of ORCA for the larger Li-Al heterobimetallic dimetallocene.

The ORCA calculations were performed on a high-performance workstation equipped with an AMD processor comprising 16 physical CPU cores (NUMA node 0: CPUs 0–15), 32 MiB L3 cache and 125 GiB RAM. The system further included an NVIDIA graphics processing unit with device ID 2704 and revision A1. AMD-V virtualisation support was enabled. This hardware configuration provided sufficient computational resources and memory bandwidth for the demanding QZVP calculations and enabled substantially shorter calculation times than the corresponding Gaussian calculations performed on standard laboratory workstations. The resulting computational efficiency supported the use of ORCA for the subsequent calculations of the Li-Al heterobimetallic dimetallocene.

Conclusion and Outlook

This study demonstrates that DFT calculations combined with the GIAO formalism at the B3LYP/TZVP level provide a reliable computational workflow for the prediction of ^{13}C and ^{1}H NMR chemical shifts in chemically diverse aromatic and organometallic systems. For the aromatic reference compounds, the calculated chemical shifts showed close agreement with experimental data, and linear regression-based scaling further reduced systematic deviations. The additional validation using ferrocene, acetylferrocene and lithium cyclopentadienide provided external experimental support for the transferability of the workflow to selected metal-containing systems.

For the Li/Al target compounds, complete atom-resolved ^{13}C and ^{1}H datasets under directly comparable experimental conditions were not available for all systems. Therefore, Gaussian 09 and ORCA 6.0.1 calculations were compared as an internal consistency check. The close agreement between both software packages demonstrated high cross-platform numerical reproducibility of the calculated ^{13}C and ^{1}H chemical shifts. This result supports the robustness of the computational implementation, although it does not replace direct experimental validation.

A key finding of this study is that the larger QZVP basis set did not provide a meaningful improvement in

predictive accuracy for the investigated reference systems. In contrast, TZVP yielded comparable or lower mean absolute errors for both ^{13}C and ^{1}H chemical shifts while requiring substantially shorter computation times. The QZVP calculations increased the computational demand by up to more than two orders of magnitude, depending on the molecular system. These results establish TZVP as a practical basis set for balancing predictive performance and computational cost in routine DFT-based NMR calculations.

The novelty of the present work lies in the direct evaluation of aromatic and organometallic benchmark systems using a consistent computational workflow, combined with a systematic comparison of basis-set performance and cross-platform reproducibility. The results demonstrate that the B3LYP/TZVP/GIAO approach can provide chemically meaningful and reproducible NMR predictions for structurally diverse systems. The workflow is therefore particularly useful when experimental NMR data are incomplete, difficult to assign or unavailable for direct comparison.

Future work could expand the approach to additional NMR-active nuclei, including ^{15}N, ^{19}F and ^{31}P, thereby extending its application to molecular systems relevant to catalysis, bioinorganic chemistry and pharmaceutical development. The inclusion of explicit solvent molecules or hybrid quantum mechanics/molecular mechanics (QM/MM) approaches could improve the description of hydrogen bonding, ion pairing and conformational flexibility, particularly for polar or highly solvated systems. Machine-learning-assisted scaling functions trained on curated experimental datasets may further reduce residual systematic deviations without substantially increasing computational cost. Finally, coupling DFT-based NMR prediction workflows with automated structure-generation and screening frameworks could enable high-throughput virtual NMR libraries for the discovery, structural verification and prioritisation of novel compounds in academic and industrial research.

References

1 Claridge T D W, *High-Resolution NMR Techniques in Organic Chemistry*, 3rd Ed., (Elsevier), 2016.

2 Bischoff I-A, Danes S, Thoni P, Morgenstern B, Andrada D M, Muller C, Lambert J, Giebelmann E C J, Zimmer M & Schafer A, *Nat Chem*, 16 (2024) 1093.

3 Lodewyk M W, Siebert M R & Tantillo D J, *Chem Rev*, 112 (2012) 183.

4 Venianakis T, Oikonomaki C, Siskos M G, Varras P C, Primikyri A, Alexandri E & Gerothanassis L P, *Molecules*, 25 (2020) 3660.

5 Cheeseman J R, Trucks G W, Keith T A & Frisch M J, *J Chem Phys*, 104 (1996) 5497.

6 Safi Z S & Wazzan N, *Sci Rep*, 12 (2022) 17798.

7 Kondrashova S A & Latypov S K, *Molecules*, 29 (2024) 6052.

8 Jonas E, Kuhn S A & Schlörer N, *Magn Reson Chem*, 60 (2022) 1021.

9 Weigend F & Ahlrichs R, *Phys Chem Chem Phys*, 7 (2005) 3297.

10 Weigend F, *Phys Chem Chem Phys*, 8 (2006) 1057.

11 Frisch M J, Trucks G W, Schlegel H B, Scuseria GE, Robb MA, Cheeseman JR, Scalmani G, Barone V, Mennucci B, Petersson GA, Nakatsuji H, Caricato M, Li X, Hratchian HP, Izmaylov AF , Bloino J, Zheng G, Sonnenberg JL, Hada M, Ehara M, Toyota K, Fukuda R, Hasegawa J, Ishida M, Nakajima T, Honda Y, Kitao O, Nakai H, Vreven T, Montgomery JA, Peralta JE, Ogliaro F, Bearpark M, Heyd JJ, E Brothers, Kudin KN, Staroverov VN, Kobayashi R, Normand J, Raghavachari K, Rendell PG, Burant JC, Iyengar SS, Tomasi J, Cossi M , Rega N, Millam JM, Klene M, Knox JE, Cross JB, Bakken V, Adamo C, Jaramillo J, Gomperts R, Stratmann R E, Yazyev O, Austin A J, Cammi R, Pomelli C, Ochterski J W, Martin R L, Morokuma K, Zakrzewski V G , Voth G A, Salvador P, Dannenberg JJ, Dapprich S, Daniels A D, Farkas O, Foresman JB, Ortiz JV, Cioslowski J & Fox DJ, *Gaussian 09*, Revision D.01 (Gaussian Inc, Wallingford CT), 2013.

12 Neese F, Wennmohs F, Becker U & Riplinger C, *J Chem Phys*, 152 (2020) 224108.

13 Neese F, *WIREs Comp Mol Sci*, 2 (2012) 73.

14 Friebolin H, *Basic One- and Two-Dimensional NMR Spectroscopy*, 4 (2005) 1030.

15 Hohenberg P & Kohn W, *Phys Rev*, 136 (1964) 864.

16 Ramachandran K I, Gopakumar D & Namboori K, *Comp Chem Mole Mode: Principles App,* (2008) 171.

17 Stephens P J, Devlin F J, Chabalowski C F & Frisch M J, *J Phys Chem*, 98 (1994) 11623.

18 Becke A D, *J Chem Phys*, 98 (1993) 5648.

19 Lee C, Yang W & Parr R G, *Phys Rev B*, 37 (1988) 785.

20 Vosko S H, Wilk L & Nusair M, *Can J Phys*, 58 (1980) 1200.

21 London F, *J Phys Radium*, 8 (1937) 397.

22 McWeeny R, *Phys Rev*, 126 (1962) 1028.

23 Ditchfield R, *Mol Phys*, 27 (1974) 789.

24 Wolinski K, Hinton J F & Pulay P, *J Am Chem Soc*, 112 (1990) 8251.

25 Bursch M, Mewes J-M, Hansen A & Grimme S, *Angew Chem Int Ed*, 61 (2022) e202205735.

26 Tomasi J, Mennucci B & Cammi R, *Chem Rev*, 105 (2005) 2999.

27 Scalmani G & Frisch M J, *J Chem Phys*, 132 (2010) 114110.

28 Improta R, Scalmani G, Frisch M J & Barone V, *J Chem Phys*, 127 (2007) 074504.

29 Improta R, Barone V, Scalmani G & Frisch M J, *J Chem Phys*, 125 (2006) 054103.

30 Hesse M, Meier H & Zeeh B, *Spektroskopische Methoden in der organischen Chemie*, (2012).

31 SDBSWeb, *National Institute of Advanced Industrial Science and Technology*, https://sdbs.db.aist.go.jp/CompoundLanding.aspx?sdbsno=7071.

32 PubChem, Compound Summary for CID 241, *National Center for Biotechnology Information*, https://pubchem.ncbi.nlm.nih.gov/compound/241.

33 PubChem, Compound Summary for CID 996, *National Center for Biotechnology Information*, https://pubchem.ncbi.nlm.nih.gov/compound/996.

34 PubChem, Compound Summary for CID 1140, *National Center for Biotechnology Information*, https://pubchem.ncbi.nlm.nih.gov/compound/1140.

35 PubChem, Compound Summary for CID 6115, *National Center for Biotechnology Information*, https://pubchem.ncbi.nlm.nih.gov/compound/6115.

36 PubChem, Compound Summary for CID 6396, *National Center for Biotechnology Information*, https://pubchem.ncbi.nlm.nih.gov/compound/6396.

37 PubChem, Compound Summary for CID 7416, *National Center for Biotechnology Information*, https://pubchem.ncbi.nlm.nih.gov/compound/7416.

38 Hanwell M D, Curtis D E, Lonie D C, Vandermeersch T, Zurek E & Hutchison G R, *J Cheminform*, 4 (2012) 17.

39 R Core Team, *R: A Language and Environment for Statistical Computing* (R Foundation for Staistical Computing, Vienna), 2023.

40 The MathWorks Inc, *MATLAB version 9.12.0 (R2022a)* (The MathWorks Inc, Natick MA), 2022.

41 Bland J M & Altman D G, *Lancet*, 1 (1986) 307.

42 Verma R P & Hansch C, *Chem Rev*, 111 (2011) 2865.

43 Wang L, Cao C & Cao C, *Magn Reson Chem*, 53 (2015) 520.

44 Weigend F, Furche F & Ahlrichs R, *J Chem Phys*, 119 (2003) 12753.